Modeling and Simulation of a Two-Mass Resonant System with Speed Controller

Ghazanfar Shahgholian, *Member, IACSIT*

***Abstract*—The dynamic analysis and application of a PID controller with compensation to a two-pass resonant system is presented. A complete state-space mathematical model for systm is first developed. Then, a PID controller with feedback compensation is designed to regulate the speed of the system. The parameters of the controller design by coefficient diagram method.**

***Index Terms*—PID controller, speed control, cofficient diagram method.**

I. Introduction

In some industrial applications, like a steel mill drives which has a long shaft and large load side mass or a robot arm which has flexible coupling, the mechanical part of the system has very low resonant frequency. The dynamics of such a system must hence be modeled as a two-mass or multi-mass system [1], [2]. A typical configuration of steel rolling mil system is show in Fig. 1.

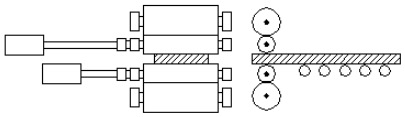

Fig. 1. A drive train with long spindle

In the design of a linear time-invariant control system using the classical control theory, the first step is to choose the controller type. In most cases, the cost of control systems increases with its complexity. Due to their merits such as simple structure, high efficiency and easy implementation, the conventional PID is widely used in most servo applications such as actuation, robotics, machine tools, and so on. They are easy to adjust and configure, in addition to providing possibilities of improvement in operation and control.

The tasks for the control of the two-mass resonant system are suppress the shaft torsional vibration, reject the effect of the load disturbance torque and tracking the load speed of the speed reference without overshoot [3]. The dynamic performances of speed and position controlled multi-mass driving system can be deteriorated especially due to the elastic coupling, non-linear friction and backlash. Many methods have been presented in the literature for the torsional vibration control of two-mass system such as sliding mode control [4], adaptive speed control [5], resonant ratio control [6] and state robust control [7]. A predictive strategy base on state feedback with a reduced order extended Kalman filter for the speed control of a two-mass system driven by a permanent magnet synchronous motor is presented in [8]. A nonlinear approach for wind power capture optimization while limiting transient loads on the drive-train components using a two-mass model and a wind speed estimator presented in [9]. In [10] proposed a Kalman filter and LQ based speed control with an integrator including load torque compensation, which Kalman filter has been used to estimate the load speed, shaft torque and load torque. A neural network estimator has been used to estimate the mechanical state variables such as the torsional torque and load-side speed of the two-mass drive system in [11].

The objective of this paper is to develop an algorithm to design a speed control strategy of a two-mass resonant system by a PID controller. It is seen that the control system has fast speed response and robust stability. This paper describes a study on the PID controller design of two-mass resonant system considering the response frequency and response step.

Manuscript received September 20, 2012; revised October 30, 2012.

Gh. Shahgholian is with the Department of Electrical Engineering, Najafabad Branch, Islamic Azad University, Esfahan, Iran (e-mail: shahgholian@iaun.ac.ir).

II. Mathematical Model

Fig. 2 shows a schematic of a two-mass resonant system consisting of two lumped inertias J_M and J_L, representing the motor and load, respectively, coupled via a shaft of finite stiffness K_S, that is subject to torsional torque T_S and excited by a combination of electromagnetic torque T_M and load-torque perturbations T_L. The motor angular velocity is denoted ω_M and the load velocity is denoted ω_L [12]. The nominal parameters of the system show in Table I.

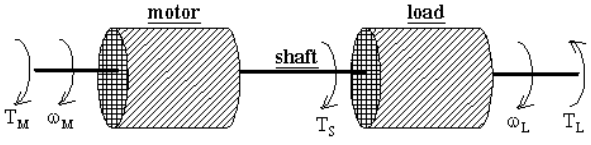

Fig. 2. Two-mass drive system

TABLE I: Nominal Parameters of the Two-Mass Plant

Symbol	Quantity	Value
K_S	shaft stiffness	30 Nm/rad
B_S	shaft damping coefficient	0.2 Nm/rad/s
J_M	motor inertia	0.02 kg.m^2
B_M	motor viscosity coefficient	0.002 Nm/rad/s
J_L	load inertia	0.165 kg.m^2
B_L	load viscosity coefficient	0.007 Nm/rad/s

The state equation of two-mass resonant system is as follows [13]:

$$\frac{d}{dt}\omega_M = -\frac{B_M}{J_M}\omega_M - \frac{1}{J_M}T_S + \frac{1}{J_M}T_M \quad (1)$$

$$\frac{\mathrm{d}}{\mathrm{dt}}\mathrm{T_S} = (\mathrm{K_S} - \frac{\mathrm{B_M B_S}}{\mathrm{J_M}})\omega_\mathrm{M} - (\mathrm{K_S} - \frac{\mathrm{B_L B_S}}{\mathrm{J_L}})\omega_\mathrm{L}$$

$$-B_S(\frac{1}{J_M} + \frac{1}{J_L})T_S + \frac{B_S}{J_M}T_M + \frac{B_S}{J_L}T_L \quad (1)$$

$$\frac{d}{dt}\omega_L = -\frac{B_L}{J_L}\omega_L + \frac{1}{J_L}T_S - \frac{1}{J_L}T_L \quad (2)$$

The transfer function load is denoted $G_L(s)$ and the transfer function motor is denoted $G_M(s)$. Fig**.** 3 provide a dynamic block diagram representation of the two-mass mechanical system which the electromagnetic torque produced by the servo machine. The machine rotor angular velocity, load angular velocity and torsional torque can be derived, such as:

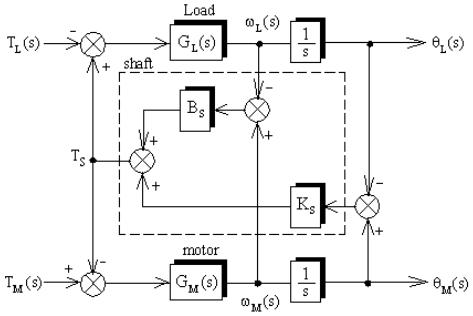

Fig. 3. Block diagram of two-mass drive system

$$H_{LM}(s) = \frac{\omega_L(s)}{T_M(s)}\bigg|_{T_L=0} = \frac{1}{J_L J_M}\frac{B_S s + K_S}{\Delta(s)} \quad (3)$$

$$H_{MM}(s) = \frac{\omega_M(s)}{T_M(s)}\bigg|_{T_L=0} = \frac{1}{J_L J_M}\frac{J_L s^2 + (B_L + B_S)s + K_S}{\Delta(s)} \quad (4)$$

$$H_{SM}(s) = \frac{T_S(s)}{T_M(s)}\bigg|_{T_L=0} = \frac{1}{J_L J_M}\frac{(B_S s + K_S)(J_L s + B_L)}{\Delta(s)} \quad (5)$$

where the characteristic equation of the open loop system is given as:

$$\Delta(s) = s^3 + (\frac{B_M + B_S}{J_M} + \frac{B_L + B_S}{J_L})s^2 + (\frac{K_S(J_M + J_L) + B_S(B_M + B_L) + B_M B_L}{J_M J_L})s + \frac{K_S(B_M + B_L)}{J_M J_L} \quad (6)$$

Since damping losses usually considered being relatively low, they are neglected without significantly affecting the accuracy of the forgoing analysis. The resonance frequency (ω_R) and anti-resonance (ω_A) frequency are defined as:

$$\omega_A = \sqrt{\frac{K_S}{J_L}} \quad (7)$$

$$\omega_R = \omega_A\sqrt{1 + \frac{J_L}{J_M}} \quad (8)$$

An increase in the motor inertia constant decreases the ω_R without affecting the ω_A. Conversely, increasing the K_S coefficient increases both ω_R and ω_A. Therefore, in the large systems, which have large inertias, generally produce low natural frequencies. The dominant eigenvalues for open-loop system are P_1=-0.0468 and $p_{2,3}$=-5.6529±j40.6185. The resonant frequency is ω_R=41.0 rad/s and anti-resonant frequency is ω_A=13.5 rad/s. The damping factor of the original plant without the controller is η=0.1367. Since all eigenvalues of the system are on the left hand of the plane, the system is stable but highly damped. The response frequency of transfer functions relative to motor torque show in Fig. 4.

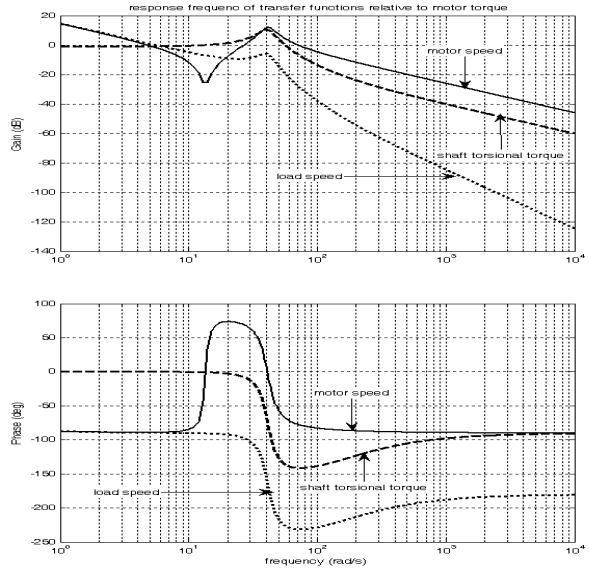

Fig. 4. The response frequency of transfer function relative to motor

III. Controller Design

The Coefficient Diagram Method (CDM) is an indirect pole placement method to design an appropriate characteristic polynomial. The CDM can give a controller design which is both stable and robust, and it has the desired system response speed. CDM needs some design parameters with respect to the characteristic polynomial coefficients which are the equivalent time constant (τ) and the stability index (γ_k) [14, 15]. A general form of characteristic polynomial of a closed-loop control system is:

$$\Delta(s) = a_n s^n + a_{n-1}s^{n-1} + \ldots + a_1 s + a_0 = \sum_{k=1}^{n} a_k s^k \quad (9)$$

There is a relationship among the coefficients of the controlled system closed-loop characteristic polynomial:

$$a_k = \frac{a_o \tau^k}{\gamma_{k-1}\gamma_{k-2}^2 \cdots \gamma_1^{k-1}} \quad (10)$$

In this section, design considerations of the proposed controllers combined with feedback compensation are given. Fig. 5 show a close-loop control with PID controller, $G_V(s)= K_{PS}+ K_{IS}/s+sK_{DS}$, and feedback compensation, $G_F(s)=K_{PF}+ K_{IF}/s +sK_{DF}$. The motor speed, shaft torque and motor torque are represented as:

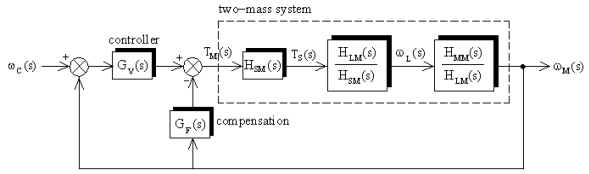

Fig. 5. Control structure of a two-mass drive system in Simulink/Matlab

$$\omega_M(s) = H_{VF}(s)\,\omega_C(s) - H_{TF}(s)\,T_L(s) \quad (11)$$

$$T_S(s) = H_{SR}(s)\,\omega_C(s) - H_{ST}(s)\,T_L(s) \quad (12)$$

$$T_M(s) = H_{MR}(s)\,\omega_C(s) - H_{MT}(s)\,T_L(s) \quad (13)$$

The closed-loop transfer function from the command speed (ω_C) to the motor speed and the from the command speed to the disturbance torque are:

$$H_{VF}(s) = \frac{\omega_M(s)}{\omega_C(s)}\bigg|_{T_L(s)=0} = \frac{G_V(s)\,H_{MM}(s)}{1+[G_V(s)+G_F(s)]\,H_{MM}(s)} \quad (14)$$

$$H_{TF}(s) = -\frac{\omega_M(s)}{T_L(s)}\bigg|_{\omega_C(s)=0} = \frac{H_{ML}(s)}{1+[G_V(s)+G_F(s)]\,H_{MM}(s)} \quad (15)$$

The closed-loop transfer function from the ω_C to the motor torque and from the ω_C to the shaft torque is:

$$H_{TR}(s) = \frac{T_M(s)}{\omega_C(s)}\bigg|_{T_L(s)=0} = \frac{G_V(s)}{1+[G_V(s)+G_F(s)]\,H_{MM}(s)} \quad (16)$$

$$H_{SR}(s) = \frac{T_S(s)}{\omega_C(s)}\bigg|_{T_L(s)=0} = \frac{H_{SM}(s)[1+G_F(s)\,H_{MM}(s)]}{1+[G_V(s)+G_F(s)]\,H_{MM}(s)} \quad (17)$$

The closed loop characteristic polynomial in close-loop with controller is given by:

$$\Delta_{PID-COM}(s) = (K_{DS}+K_{DF}+J_M)s^4 + (K_{PS}+K_{PF})s^3 + (J_M\,\omega_R^2 + K_{IS} + K_{IF} + K_{DS}\,\omega_A^2 + K_{DF}\,\omega_A^2)s^2 + (K_{PS}\,\omega_A^2 + K_{PF}\,\omega_A^2)s + (K_{IS}\,\omega_A^2 + K_{IF}\,\omega_A^2) \quad (18)$$

Therefore, the closed-loop characteristic equation of the system with only PID controller is similar to that of the system with PID controller and compensation. The zeros of the H_{VF}(s) depend on not only anti-resonance but also the variation of forward controller gains, while the zeros of transfer function are independent of compensation gains. But the zeros of H_{VT}(s) are independent on the controller gains and compensation gains.

In I-PD controller, the controller structure consists of an integral controller in forward (K_{DS}=0, K_{PS}=0) and proportional derivative compensation (K_{IF}=0). If E_V is output signal of integral controller, the state-space equations of the system with I-PD controller are given by:

$$\frac{d}{dt}E_V = K_{IS}(\omega_C - \omega_M) \quad (19)$$

$$\frac{d}{dt}\omega_M = \frac{1}{J_M + K_D}[E_V - T_S - (B_M + K_{PS})\,\omega_M] \quad (20)$$

$$\frac{d}{dt}\omega_L = \frac{-B_L}{J_L}\omega_L + \frac{1}{J_L}T_S - \frac{1}{J_L}T_L \quad (21)$$

$$\frac{d}{dt}T_S = [K_S - \frac{B_S\,(B_M + K_P)}{J_M + K_D}]\omega_M + [-K_S + \frac{B_S\,B_L}{J_L}]\omega_L - (\frac{B_S}{J_M + K_D} + \frac{B_S}{J_L})T_S + \frac{B_S}{J_L}T_L \quad (22)$$

With compared the polynomial coefficients of characteristic equation in PID controller with compensation and CDM the equivalent time constant and PID controller's gains can be found as following:

$$\tau = \frac{\gamma_1\sqrt{\gamma_2}}{\omega_A} \quad (23)$$

$$K_I = K_{IS} + K_{IF} = \frac{K_S\,\gamma_3}{\gamma_1\gamma_2\gamma_3 - \gamma_1 - \gamma_3} \quad (24)$$

$$K_D = K_{DS} + K_{DF} = \frac{J_L\,\gamma_1}{\gamma_1\gamma_2\gamma_3 - \gamma_1 - \gamma_3} - J_M \quad (25)$$

$$K_P = K_{PS} + K_{PF} = \frac{\gamma_1\gamma_3\sqrt{K_S\,J_L}\sqrt{\gamma_2}}{\gamma_1\gamma_2\gamma_3 - \gamma_1 - \gamma_3} \quad (26)$$

In order to achieve system stability on base Routh-Hurwitz algorithm, the condition for stability index for a four order system is:

$$\gamma_2 > \frac{1}{\gamma_1} + \frac{1}{\gamma_3} \quad (27)$$

IV. Simulation Results

In this section, we verify the validity of the proposed method. All simulation is executed by Matlab. Fig. 6 show a close-loop control with PID controller and feedback compensation, structure in Simulink/Matlab. The parameters of the controller obtained from (19)-(22) are summarized in Table II. The eigenvalues of the close-loop system are listed in Table III. Fig. 7 and 8 show the step response of motor

speed and frequency response for change in stability indexes with PID controller. The simulation results of motor speed and load speed due to unit-step command speed when the two-mass system is compensated by the conventional PID controller, I-PD controller and PID-P controller show in Figs. 9 and 10, respectively.

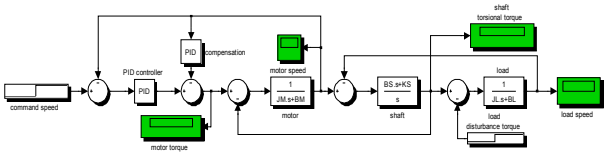

Fig. 6. Control structure of a two-mass drive system in Simulink/Matlab

TABLE II: CONTROLLER PARAMETERS

Stability index	K_P	K_I	K_D	τ
γ_1=4, γ_2=2.5, γ_3=2.5	1.9015	4.0541	0.0157	0.4690
γ_1=4, γ_2=2.5, γ_3=2.5	5.2440	20.0000	0.2550	0.2622
γ_1=4, γ_2=2.5, γ_3=2.5	7.0791	27.2727	0.1900	0.2596

TABLE III: EIGENVALUE OF THE CLOSE-LOOP SYSTEM

Stability index	Eigenvalue
γ_1=4, γ_2=2.5, γ_3=2.5	-18.06±j12.08, -14.07, -3.1
γ_1=4, γ_2=2.5, γ_3=2.5	-2.74±j14.99, -6.79±j3.29
γ_1=4, γ_2=2.5, γ_3=2.5	-2.42±j13.63, -5.21, -23.67

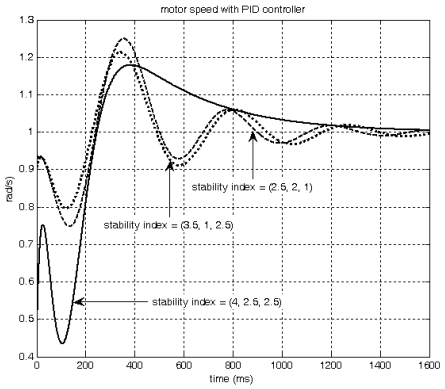

Fig. 7. The parameter effect of PID controller on motor speed

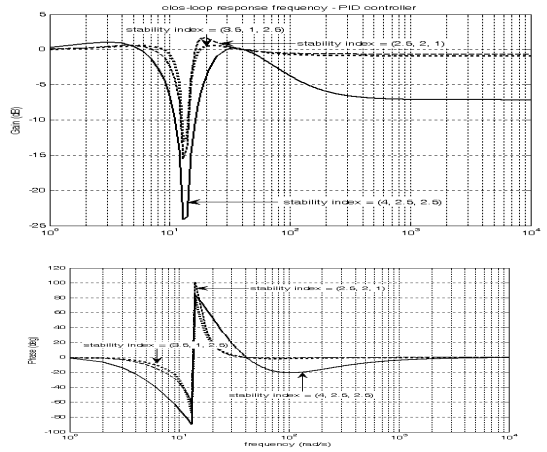

Fig. 8. The parameter effect of PID controller on frequency response

The simulation results of shaft torque and motor torque due to unit-step command speed when the two-mass system is compensated by the conventional PID controller, I-PD controller and PID-P controller show in Figs. 11 and 12, respectively.

The simulation results of shaft torque and motor speed due to unit-step command speed using I-PD controller in the two-mass system with load inertia deviations show in Fig. 13 and 14, respectively. It is shown that the controller yields a robust stability system.

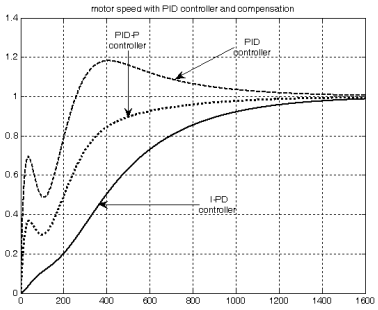

Fig. 9. Step response of motor speed with PID controller and compensation

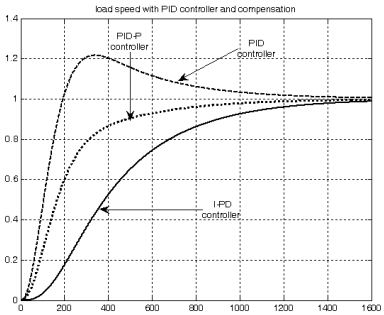

Fig. 10. Step response of load speed with PID controller and compensation

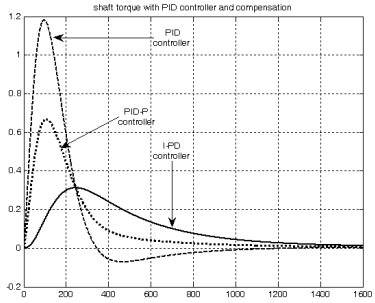

Fig. 11. Step response of shaft torque with PID controller and compensation

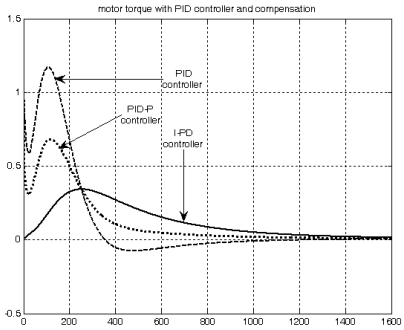

Fig. 12. Step response of motor torque with PID controller and compensation

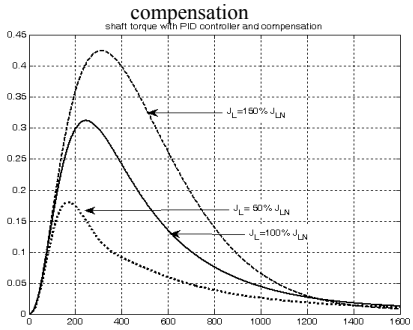

Fig. 13. Step response of shaft torque using I-PD controller with load inertia deviations

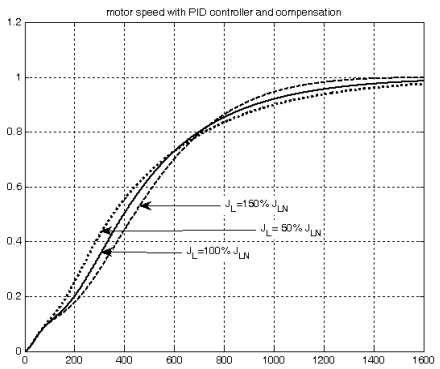

Fig. 14. Step response of motor speed using I-PD controller with load inertia deviations

V. Conclusion

Vibration suppression and attainment of robustness in motion control systems is an important problem in industry applications. The response of the system is studied for command speed changes. Analysis and simulation results are illustrated to verify good performance obtained using the proposed controller.

References

[1] J. Wang, Y. Zhang, L. Xu, Y. Jing, and S. Zhang, "Torsional vibration suppression of rolling mill with constrained model predictive control," *IEEE/ VVICA*, vol. 2, pp. 6401-6405, June 2006.

[2] G. Shahgholian and P. Shafaghi, "Simple analytical and robust controller design for two-mass resonant system," *IEEE/ICCEE*, pp. 245-248, Dec. 2009.

[3] Y. S. Kim, S. B. Kim, J. S. Kim, C. H. Yoo', and H. J.Kim, "Two degree of freedom speed control of induction motor having two mass resonant system," *IEEE/IECON*, vol. 2, pp. 1210-1215, Aug. 1996.

[4] K. Erenturk, "Nonlinear two-mass system control with sliding-mode and optimized proportional-integral derivative controller combined with a grey estimator," *IET Contr. The. Apll.*, vol. 2, no. 7, pp. 635-642, 2008.

[5] H. Schuster, C. Westermaier, and D. Schroder, "Non-identifier-based adaptive speed control for a two-mass flexible servo system: consideration of stability and steady state accuracy," *IEEE/MED*, pp. 1-6, 2006.

[6] T. M. O'Sullivan, C. M. Bingham, and N. Schofield, "High performance control of dual-inertia servo drive systems using low cost integrated SAW torque transducers," *IEEE Tran. on Ind. Elec.*, vol. 55, no. 4, pp. 1226-1237, Aug. 2006.

[7] K. Peter, I. Scholing, and B. Orlik, "Robust output feedback H_∞ control with a nonlinear observer for a two-mass system," *IEEE Trans. Ind. Appl.*, vol. 6, no. 2, pp. 637-644, 2003

[8] E. J. Fuentes, C. A. Silva, and J. I. Yuz, "Predictive Speed Control of a Two-Mass System Driven by a Permanent Magnet Synchronous Motor," *IEEE Trans. on Ind. Ele.*, vol. 59, no. 7, pp. 2840-2848, 2012.

[9] B. Boukhezzar and H. Siguerdidjane, "Nonlinear control of a variable-speed wind turbine using a two-mass model," *IEEE Trans. on Ene. Con.*, vol. 26, no. 1, pp. 149-162, 2011.

[10] J. K. Ji and S. K. Sul, "Kalman filter and LQ based speed controller for torsional vibration suppression in a 2-mass motor drive system," *IEEE Trans. Ind. Ele.*, vol. IE-43, no. 6, pp. 564-571, Dec. 1995.

[11] T. O. Kowalska and K. Szabat, "Neural network application for mechanical variables estimation of a two-mass drive system," *IEEE Tran. Ind. Electron.*, vol. 54, no. 3, pp. 1352-1364, 2007.

[12] O. Ocal, M. T. SOylemez, and A. Bir, "Robust pole assignment using coefficient diagram method," *ACSE*, Dec. 2005.

[13] G. Shahgholian, M. Zinali, P. Shafaghi, and M. H. Rezaei, "Analysis and design of torque control strategy for two-mass resonant system only by a PID controller," *ICEEDT*, Oct./Nov. 2009.

[14] G. Shahgholian, P. Shafaghi, M. Zinali, and S. Moalem, "State space analysis and control design of two-mass resonant system," *IEEE/ICCEE*, pp. 668-672, Dec. 2009.

[15] G. Shahgholian and J. Faiz, "An analytical approach to synthesis and modeling of torque control strategy for two-mass resonant systems," *Int.* Revi*. of Auto. Cont. (IREACO)*, vol. 2, no. 4, pp. 459-468, July 2009.

Ghazanfar Shahgholian was born in Esfahan, Iran, on Dec. 7, 1968. He graduated in electrical engineering from Isfahan University of Technology (IUT), Esfahan, Iran, in 1992. He received the M.Sc and PhD in electrical engineering from University Tabriz, Tabriz, Iran in 1994 and Science and Research Branch, Islamic Azad University, Tehran, Iran, in 2006, respectively. He is now an associate professor at Department of Electrical Engineering, Faculty of Engineering, Islamic Azad University Najafabad Branch. He is the author of 100 publications in international journals and conference proceedings. His teaching and research interests include application of control theory to power system dynamics, power electronics and power system simulation.